Bitlis Eren Üniversitesi Fen Bilimleri Dergisi
BİTLİS EREN UNIVERSITY JOURNAL OF SCIENCE
ISSN: 2147-3129/e-ISSN: 2147-3188
VOLUME: 12 NO: 4 PAGE: 1094-1104 YEAR: 2023
DOI:10.17798/bitlisfen.1337326

Development of Chip Temperature and Cost-Based Optimum Design for a Radial Heat Sink Cooling High Power LEDs

Orhan KALKAN[1*]

[1]*Erzincan Binali Yıldırım University, Faculty of Engineering and Architecture, Department of Mechanical Engineering, Erzincan, Turkey*
(ORCID: 0000-0002-9664-1819)

Keywords: High power LEDs, thermal management, optimization, numerical analysis

Abstract
High-power Light Emitting Diodes (LED)s are preferred in places that produce intense light output and have overheating problems because they work with high currents. Therefore, efficient thermal management is essential to ensure optimal performance and longevity. In the present study, a numerical analysis is conducted on a high-power Light Emitting Diode (LED) circuit with a Circuit on Board (COB) design featuring a radial heat sink. Additionally, a multi-objective optimization approach using the Desirability Function Approach (DFA) is introduced for the modeled radial heat sink. Two performance parameters, namely the maximum junction temperature and the cost of the radial heat sink, are defined as the objective functions, and the aim is to minimize both of these parameters. The independent variables for the objective functions are the geometrical parameters of the radial heat sink, namely the base radius (R), fin length (L), and heat sink height (H). The Response Surface Method (RSM) is applied to minimize sample numbers in the Design of Experiment (DOE) while still obtaining accurate response values. Furthermore, Analysis of Variance (ANOVA) is utilized to assess the fit of the real response equations with the representative answer equations. The minimum prediction R^2 is calculated to be 0.9748%, indicating a good agreement between the models. A cost-based, realistic optimum design for radial heat sinks, which are frequently used for COB HPLEDs, is presented in the study. The response values for this optimal design are validated with a low error rate of 0.25% using numerical analysis.

1. Introduction

Light Emitting Diodes, abbreviated as LED, are semiconductor elements that emit light when an electric current is passed through them. They are a type of solid-state lighting technology that is highly preferred in industry and daily life due to their efficiency, durability, and versatility in various applications. LEDs have revolutionized lighting technology and are used in a wide range of devices and systems, from small indicator lights to large outdoor displays. [1]. Chip-on-Board (COB) LEDs are a type of high-power LED technology that offers several advantages over traditional discrete LEDs. In a COB LED package, multiple LED chips are mounted directly onto a single substrate, forming a single module, or "chip," that acts as a single light source [2]. COB LEDs are generally more energy-efficient than traditional lighting sources like incandescent bulbs, making them an attractive option for various applications [3], [4].

COB LEDs need improved thermal performance compared to traditional discrete LEDs. Because the LED chips are mounted close together, they can share a larger heat sink area, requiring more effective heat dissipation to achieve lower operating temperatures. LEDs are energy-efficient light sources, but they still produce heat when converting

*Corresponding author: *orhan.kalkan@erzincan.edu.tr*
Received: 03.08.2023, Accepted: 17.11.2023

electricity into light. If this heat is not effectively removed, it can negatively impact the LED's performance, reliability, and lifespan. A heat sink is often used to dissipate the heat produced by light-emitting diodes (LED)s during operation. Some current studies about cooling LEDs are summarized as follows:

Song et al. focused on analyzing the cooling capabilities of a heat sink that has perforated fins. They aimed to enhance the cooling performance by investigating the impact of varying the size and number of perforations. The results revealed that a higher number of perforations with smaller sizes contributed to better cooling performance. Additionally, the research involved a numerical analysis of the heat-dissipation performance, considering factors such as fin number, fin angle, heat sink angle, and the Rayleigh number. [5]. Xu introduced a rectangular radial fin-equipped heat sink designed for high power LEDs (HPLED)s cooling. The optimization study, which aims to minimize maximum temperature and mass, considers the number of fins and fin length as parameters. The multi-objective optimization study identifies a solution with a maximum temperature of 67.7°C, a thermal resistance of 0.45 K/W, and a mass of 1.74 kg. This optimal solution corresponds to 23 fins and a fin length of 59 mm, effectively dissipating 92 W of heat [6]. Azarifar et al. explored the enhancements in both optical and thermal aspects achieved through a novel package-level liquid coolant encapsulation designed to specifically target heat generation. As a result of the study, the potential of this new cooling method for optoelectronic components was demonstrated. A remarkable minimization of 15% in thermal resistance was obtained [7]. Jiu et al. proposed a novel heat sink design equipped with a mini heat pipe array (MHPA), addressing the existing challenges in heat dissipation. The heat sink's thermal performance was thoroughly evaluated through experimental testing. With an input power of 100 W, the substrate temperature can be effectively reduced below 70 °C. The MHPA exhibits excellent temperature uniformity, with maximum temperature drops of only 0.6 °C and 1.1 °C in the vertical direction for input powers of 100 W and 200 W, respectively [8]. Ben Hamida et al. aimed to provide effective thermal management for the efficient removal and dissipation of the heat produced by an LED, thus ensuring its efficient and safe operation. The study explored a cost-effective solution to reduce the maximum LED temperature at junction points. The focus was on investigating the effects of square and circular holes in the heat sink. The findings indicated that two square or cylindrical holes lead to a decrease in the maximum temperature of the LED chips under different input powers. [9]. Rammohan studied to estimate the service life of High-Power Light Emitting Diodes (HPLED)s through an experimental approach. A real-time algorithm based on the Arrhenius model was employed to monitor HPLED failure. The results showed that at a junction temperature (T_j) of 25 °C, the lifetime of the HPLED was approximately 120,000 hours. However, when the maximum T_j of the HPLED reached 125 °C, the lifetime reduced significantly to 4796 hours at a maximum current of 0.45 A [10]. Moon et al. presented the development of a U-shaped single unit cooling fin aluminum flat heat pipe (AFHP) for a 100 W COB LED lamp with small dimensions (120 mm×120 mm×170 mm) and an electric connection using a socket. The U-shaped AFHP module did not exceed 900 g, is cost-effective due to the extrusion method used in its production, and was designed to be used in socket-type lamps. The junction temperature of the COB LED module was evaluated to be within 85 °C at an input power of 100 W [11]. Shin et al. introduced a novel active cooling method for Light LED applications using the ionic wind. Through analysis, it was presented that the center pole within the heat sink has no appreciable thermal effect. The optimum radius of the wire curvature and input voltage for the ionic wind were identified as 110 mm and 7.5 kV, respectively. Results demonstrated a significant improvement in the heat transfer coefficient of the heat sink by 37%, from 96.7 to 133 W/m^2K, due to the ionic wind, which was confirmed experimentally [12]. Lazarov et al. highlighted the exceptional performance of topology-optimized heat sinks when compared to lattice designs, proposing more straightforward and manufacturable pin-fin design interpretations. To address manufacturing costs, a simplified version of the optimized design is created and validated. Both numerical and experimental results show excellent agreement, confirming that the obtained designs outperform lattice geometries by over 21%. As a result, the optimized heat sinks offer a doubled life expectancy and a 50% decrease in operational costs compared to traditional lattice designs [13].

When we look at the studies in the literature on LED cooling, the researchers mostly focus on the heat sink design that provides effective cooling. The cooling performances of many different configurations of the heat sinks have been examined. In addition, geometric optimization of heat sink is also discussed. However, it seems that studies on cost-based optimization of heat sinks, which are frequently used for COBLEDs, are quite limited. This is evident in the literature on the subject. It is obvious that there is a gap in the literature on this subject.

In this study, a COB HPLED consisting of a radial heat sink is modeled and numerically analyzed. Then, a multi-objective optimization for the modeled radial heat sink is performed using the Desirability Function Approach (DFA). Studies in the literature also show that geometric parameters, maximum LED junction temperature, and mass are important criteria for finned heat emitters used for LEDs. The mass of the heat sink is an important criterion because aluminum material is generally used, and it is meaningful in terms of cost. Therefore, maximum junction temperature and radial heat sink cost are two performance parameters defined as objective functions. The goal of the multi-objective optimization procedure is to reduce both chosen performance parameters. The geometrical parameters of radial heat sink base radius, fin length, and heat sink height are defined as the independent variables of both objective functions. The Response Surface Method (RSM) is employed to reduce the number of Design of Experiment (DOE) samples while still obtaining an acceptable estimation of the response values. Then, Analysis of variance (ANOVA) is used to find out how well the real and representative answer equations fit together. Finally, a cost-based, realistic optimum design for radial heat sinks, which are frequently used for COB HPLEDs, is assessed in the present study.

2. Numerical Modeling

The cooling performance of the modeled COB HPLED and radial heat sink is numerically investigated using the ANSYS-Fluent package program. A COB HPLED is modeled with components such as an aluminum heatsink, GaN-based chips, silver paste, a silicon ring, thermal grease, and an aluminum heat slug. The geometric models and computational domains are generated using SolidWorks CAD software. Then, the mesh model of the domains is built up using the ANSYS Mesh module, and thereafter, the numerical model set-up and solutions are performed step by step. The thermophysical properties of the COB HPLED components are given in Table 1 [14]. LEDs have a 9.92 W electrical power supply. It has been calculated by Wu et al. that 80% of the electrical energy in LEDs is converted into thermal energy [14]. Therefore, 7.936 W heat generation is defined for LED domains when boundary conditions are set. Throughout thermal simulations, the scalar temperature field will be governed by the convection-diffusion equation. For this particular case, the following notation is frequently employed [15].

$$\left(\rho c_p\right)\frac{\partial T}{\partial t} = \left(\rho c_p\right)\nabla.(uT) - \nabla.(k\nabla T) + \dot{Q}_v \tag{1}$$

where ρ is material density, c_p is specific heat capacity, T is temperature, k is thermal conductivity, and $\dot{\mathbf{Q}}_\mathbf{v}$ is volumetric heat flux.

Table 1. Thermophysical properties of the components.

Component	Density	Component	Density
Heat sink (Al)	2707	896	204
GaN-based chips	6150	417	130
Silver paste	2300	671	8
Silicon ring	980	1173	0.2
Thermal grease	1180	1044	3.6
Heat slug (Al)	2707	896	204

Considering that the ambient temperature is 25 °C, a heat convection boundary condition is defined for all domain walls. Besides, the initial temperature of all domains is also 25 °C. On the other hand, the energy equation convergence criteria are set to 10^{-10}.

2.1. Geometric Model and Parameters

Radial heat sinks have fins that radiate outward from a central base, creating a circular or cylindrical shape. This design allows for efficient heat dissipation in all directions, as heat is conducted from the device to the base and then transferred to the fins, which increases the surface area for better heat transfer to the surrounding air. Radial heat sinks are commonly found in various electronic devices, including computers, laptops, HPLEDs, and other consumer electronics, where effective cooling is essential to maintain the device's performance and prolong its lifespan. The representation of the COB LED and radial aluminum heat sink geometric model and the used optimization parameters are shown in Figure 1. There are three geometrical optimization parameters for the radial heat sink. These are heat sink height (H), heat sink base radius (R), and heat sink fin length (L). The COB LED has a dimension of 33 mm×33 mm×2.1 mm. The size of the chips emitting heat and light in the COB LED is 1 mm×1 mm and has a 3×3 array. The distance between the chips is 0.5 mm.

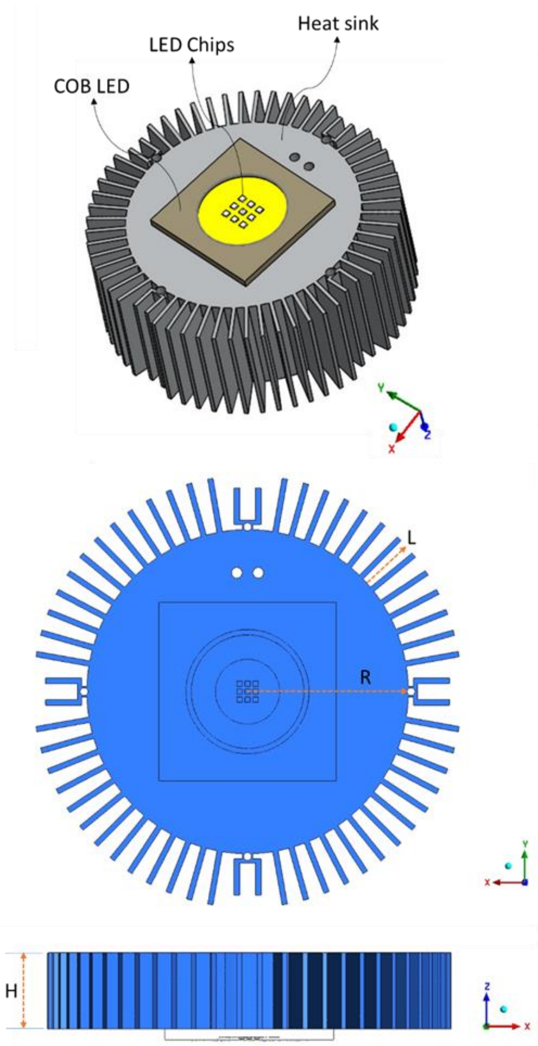

Figure 1. COB LED and heat sink model with optimization parameters.

2.2. Meshing Step

The polyhedral mesh structure is generated for the COB LED and heat sink computational domains, as depicted in Figure 2. Polyhedral meshes can require fewer elements to achieve comparable accuracy compared to traditional meshes. This can result in reduced computational effort and memory requirements for simulations. Due to the fewer element interfaces and increased geometric flexibility, polyhedral meshes may lead to improved solver behavior and convergence in some simulation scenarios [16]. While generating the mesh for the domains, the minimum element quality is not reduced below 0.2.

Mesh independency analysis is a crucial step in numerical simulations and finite element analysis to ensure that the results obtained from the simulation are not significantly affected by the size or type of the computational mesh. The purpose of this analysis is to determine the appropriate level of mesh refinement required to achieve accurate and reliable simulation results without unnecessarily increasing computational cost and time. The aim of mesh independence analysis is to strike a balance between accuracy and computational cost. If the results converge to a consistent solution as the mesh is refined, the simulation is said to be mesh-independent for the specific problem and mesh type used. Considering the present study, the maximum junction temperature ($T_{j,max}$) is selected for the mesh independency analysis parameter. Therefore, the variation of $T_{j,max}$ according to the mesh number is presented in Table 2. The mesh model has 380892 mesh numbers selected for the numerical analysis.

Table 2. Mesh independency analysis.

Mesh number	Maximum junction temperature, $T_{j,max}$ (°C)
9453	93.57
176602	88.63
380892	88.05
516841	88.04

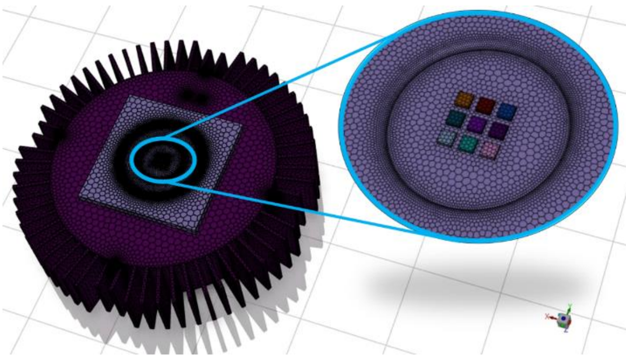

Figure 2. Mesh model of the COB LED and heat sink domains.

2.3. Validation of the Numerical Solutions

In this section, the numerical solution results of the open literature and the current study are compared for the model with the same geometric parameters and COB LED. Figure 3 shows the comparison of the temperature contours of COB LED and radial heat sinks introduced by Wu et al. and the present study [14]. H is 15 mm, R is 30 mm, and L is 10 mm for both studies. When both the chips with maximum temperatures and the heat sink temperatures are compared, it is seen that suitable results are obtained. Besides, Wu et al. validated their numerical results with an experimental study.

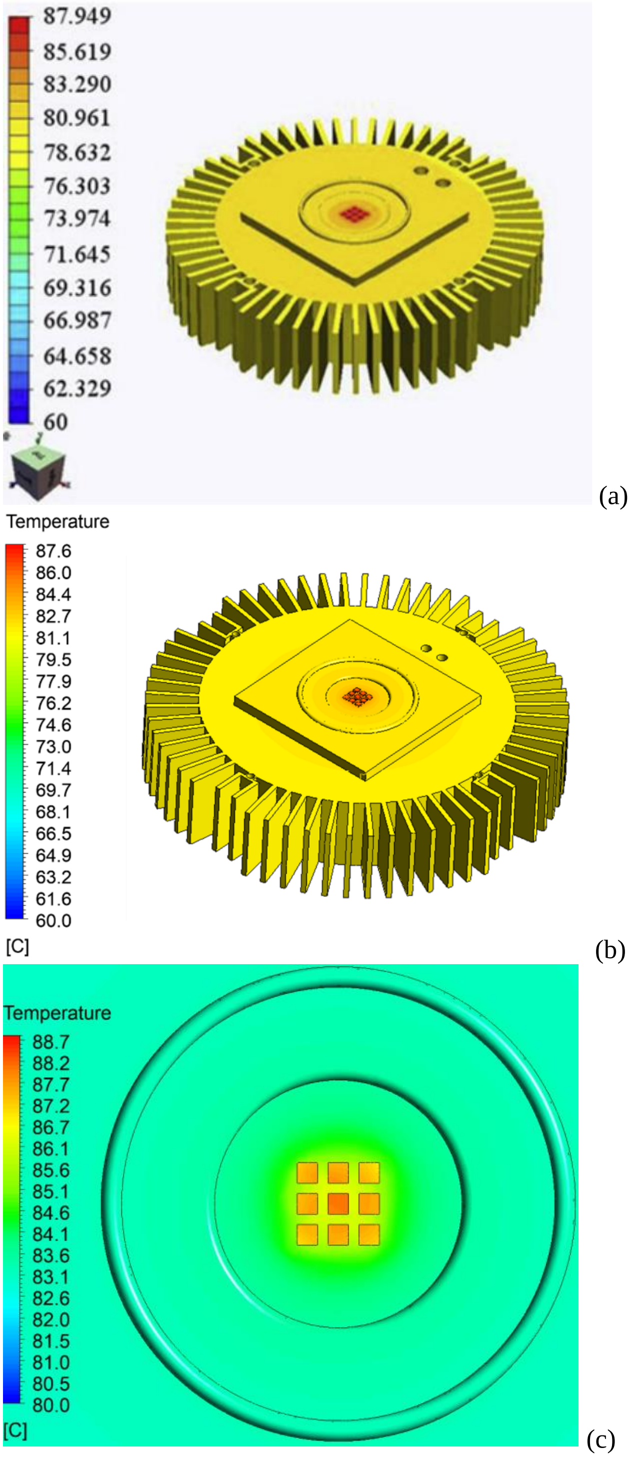

Figure 3. Temperature distributions of COB LED and heat sink presented by a) Wu et al. [14], b) this study, and c) COB LED detail in the present study.

3. Multi-Objective Optimization

In this section, $T_{j,max}$ and heat sink cost (C_{hs}) are two performance parameters defined as objective functions. The goal of the multi-objective optimization procedure is to reduce both of these chosen performance parameters. The previously defined geometrical parameters of R, L, and H are the independent variables of both objective functions. These independent variables are also optimization parameters. The optimization parameters and their levels are given in Table 3.

For a full factorial DOE, 33=27 different solutions must be performed. The RSM is employed to reduce the number of DOE samples while still obtaining an acceptable estimation of the response values. The core principle of this method involves creating a simplified mathematical representation of computationally intensive analysis and simulation codes. This surrogate model replaces the original code to facilitate multi-objective design optimization [17], [18].

Configuring the response surface aims to strike a balance between accuracy and computational cost. Achieving an acceptable level of accuracy while minimizing computational effort is the primary objective. The accuracy of the response surface depends on two key factors. The first factor is the selection of the appropriate approach function, and the second factor is determining the specific design points within the design area, often referred to as DOE. Quadratic Central Composite Design is one of the most preferred methods for generating mathematical model functions. This method relies on a quadratic polynomial that establishes a straightforward correlation between the design variables and their corresponding responses. The unknown coefficients in this mathematical model are determined through the least squares method. The actual response function (g) and the approximation function (G) are given by the following equations, respectively.

Table 3. Independent variables and their levels.

Independent variables	Optimization Parameters (mm)	Levels		
		-1	0	1
I_1	R	25	30	35
I_2	L	5	10	15
I_3	H	10	55	100

$$g = f(I_1, I_2, \ldots, I_n) + E \tag{2}$$

$$G = \beta_0 + \sum_{i=1}^{m} \beta_i I_i + \sum_{i=1}^{m} \beta_{ii} {I_i}^2 + \sum_{i=1}^{m-1} \sum_{j=i+1}^{m} \beta_{ij} I_i I_j + E \tag{3}$$

Analysis of variance (ANOVA) is used to find out how well the real and representative answer equations fit together. ANOVA is a statistical technique used to compare the means of two or more groups to determine if there are any significant differences between them. ANOVA is particularly useful when comparing means from multiple groups simultaneously, making it a powerful tool for DOE and research [19], [20].

Prior to the optimization process, the interrelationship between the objective functions and the independent variables is assessed, leading to the formation of approximation equations. To evaluate the compatibility between the approximation functions and the actual objective functions, ANOVA employs several measurement tools, including the R2, adjusted R^2, adjusted R^2 ($\mathbf{R^2{}_a}$), predicted R^2 ($\mathbf{R^2{}_p}$) and Adequate Precision (AP). The relevant equations for these measurement tools are provided below.

$$R^2 = 1 - SS_e/SS_t \tag{4}$$

$$R^2{}_a = 1 - (1 - R^2)\frac{n-1}{n-p-1} \tag{5}$$

$$R^2{}_p = (1 - \sum_{i=1}^{n} e_{-i}{}^2)/SS_t \tag{6}$$

$$AP = \frac{\max(\hat{J}) - \min(\hat{J})}{\sqrt{\frac{p\varepsilon}{n}}} \tag{7}$$

here ε is the residual mean square, p is predictors number, $\hat{\boldsymbol{J}}$ is the prediction at the run, SSt is the sum of squares total, SS_e is the sum of squares error. AP value greater than 4 indicates an adequate signal. The present model can be used to navigate the design space.

The composite desirability function (CDF) approach is performed to select optimum DOE sample. A composite desirability function is a technique used in multi-objective optimization to combine multiple individual objective functions into a single overall desirability function. The purpose of using a composite desirability function is to simultaneously optimize multiple conflicting objectives by transforming them into a unified goal. The basic idea behind the composite desirability function is to assign a desirability value to each objective function based on its importance and desired target. The desirability value typically ranges from 0 to 1, where 0 represents the worst outcome (undesirable) and 1 represents the best outcome (fully desirable). Intermediate values between 0 and 1 indicate partial desirability. The individual objective functions are usually normalized to a common scale before assigning desirability values. This normalization ensures that objectives with different units or scales can be combined effectively. Once the desirability values are assigned, the composite desirability function is computed by combining the individual desirability values. There are several methods to combine these desirability values, such as taking the geometric mean, the arithmetic mean, the product of desirability values, or the minimum value among the desirability values. By maximizing the composite desirability function, the optimization process aims to find the optimal set of input variables that simultaneously satisfy the desired targets for all individual objectives. Composite desirability functions are widely used in engineering, manufacturing, and other fields where multiple conflicting objectives need to be considered simultaneously. They provide a powerful approach to handling multi-objective problems and making informed decisions when facing trade-offs between different criteria. [21]. The following desirability function handles the multi-objective optimization.

$$D = \prod_{i-1}^{n} d_i{}^{w_i \frac{1}{\sum_{i=1}^{n} w_i}} \tag{8}$$

4. Results and Discussion

A total of 15 samples are randomly generated for DOE based on the CCF approach. A separate geometry is generated for each sample, and the numerical analysis procedure is followed. The optimization parameters in each sample are calculated numerically using ANSYS-Fluent. DOE has 15 randomly generated samples, and their response values are shown in Table 4.

Then, the multi-objective optimization procedure is run to determine the optimum parameters. Quadratic approximation equations are generated for $T_{j,max}$, and C_{hs} objective functions. Next, an ANOVA is performed for both the objective function and its independent variables, which are also optimization geometric parameters. Data transformations are preferred when the range between the maximum and minimum values of the objective functions is excessively large. Data transformations are techniques used to modify the original data in order to meet specific requirements or improve the quality of the data for analysis or modeling purposes. Data transformation is a common step in data preprocessing and is often employed to address issues like data skewness and heteroscedasticity or normalize the data for certain statistical tests [22]. It is seen that the $T_{j,max}$, and C_{hs} value ranges are far from each other. Therefore, it would be logical to transform the data for $T_{j,max}$ and bring it to close value ranges with C_{hs}. Considering the present DOE dataset, an inverse data transformation for $T_{j,max}$ is generated. It is understood from Figure 4 that the actual and estimated values for both objective functions are in good agreement with each other.

Table 4. Optimization parameters and response values.

Sample no	Optimization parameters (mm)			Response values	
	R	L	H	$T_{j,max}$ (°C)	C_{hs} ($)
1	35.00	15.00	10.00	88.581	0.283
2	25.00	5.00	10.00	155.259	0.138
3	25.00	5.00	100.00	47.581	1.381
4	30.00	10.00	109.69	39.727	2.254
5	35.00	5.00	100.00	45.711	2.514
6	35.00	15.00	100.00	37.668	2.828
7	25.00	15.00	10.00	95.444	0.169
8	25.00	15.00	100.00	38.109	1.694
9	23.92	10.00	55.00	49.395	0.791
10	30.00	16.08	55.00	42.935	1.235
11	36.08	10.00	55.00	47.641	1.549
12	30.00	10.00	0.31	321.249	0.006
13	30.00	3.92	55.00	62.193	1.025
14	30.00	10.00	55.00	48.385	1.130
15	35.00	5.00	10.00	132.183	0.251

Table 5 and Table 6 represent the ANOVA test summary and fit statistics for both regression approximation equations derived for $T_{j,max}$, and C_{hs}, respectively. Model equations can estimate the response values with a minimum prediction R^2 of 0.9748%, which indicates a good fit. Besides, AP values for both objective functions are greater than 4. This also indicates good navigation for the design space.

Table 5. ANOVA test summary.

Response Model	DF	SS	MS	F-value	p-value
$T_{j,max}$	3	0.0008	0.0003	293	<0.0001
C_{hs}	6	11.41	1.90	3573	<0.0001

Table 6. ANOVA fit statistics.

Response Model	R^2	R^2_a	R^2_p	AP
$T_{j,max}$	0.9876	0.9843	0.9748	43.8384
C_{hs}	0.9996	0.9993	0.9987	178.2252

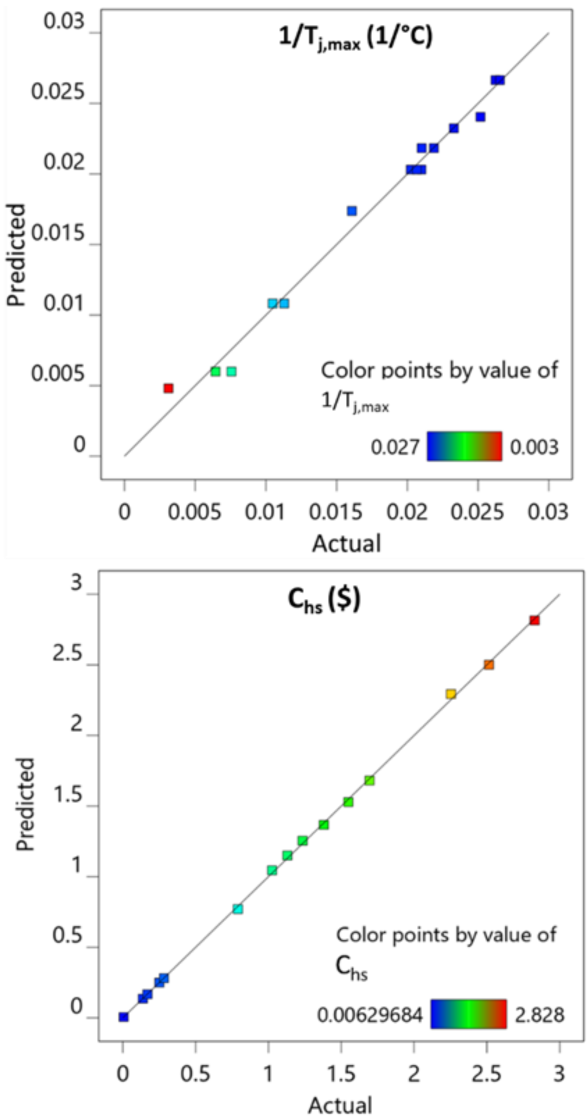

Figure 4. Actual and predicted value comparison for the objective functions.

Finally, an optimal solution set is generated using the CDF approach, as given in Table 7. The dataset in the first row with the maximum desirability value is selected as the optimum design. The heat sink with a 25 m base radius, 15 mm fin length, and 55.36 mm height is selected as the optimum radial heat sink design.

Table 7. Optimal data set.

#	R (mm)	L (mm)	H (mm)	$T_{j,max}$ (°C)	C_{hs} ($)	Desirability
1	**25**	**15**	**55.36**	**43.891**	**0.931**	**0.751**
2	25	15	55.681	43.784	0.936	0.751
3	25	15	54.998	44.014	0.924	0.751
4	25	15	54.642	44.136	0.918	0.751
5	25.008	15	56.306	43.579	0.947	0.751
6	25	15	53.764	44.444	0.904	0.751
7	25	14.967	55.81	43.771	0.937	0.751
8	25	14.962	55.444	43.899	0.931	0.751
9	25	14.935	55.048	44.058	0.924	0.751
10	25.043	15	56.125	43.638	0.946	0.751
11	25	15	52.336	44.968	0.88	0.751
12	25	14.887	56.275	43.692	0.944	0.751
13	25	14.798	56.481	43.707	0.946	0.75
14	25	15	59.823	42.511	1.006	0.75
15	25.103	15	52.683	44.838	0.892	0.75
16	25.104	15	57.903	43.076	0.98	0.75
17	25.166	15	55.229	43.935	0.939	0.749
18	25	15	61.022	42.179	1.026	0.749
19	25	14.459	53.971	44.89	0.898	0.748
20	25	14.365	55.735	44.361	0.926	0.748

The optimum design of the selection is remodeled and numerically analyzed to ensure that the response values of the optimum design parameters truly reflect the correct data. Figure 5 depicts the temperature distribution of the COB LED with a heat sink, which has an optimum design. When $T_{j,max}$ response value, and the confirmation analysis results are compared, it is seen that they are in good agreement with a 0.25% error rate.

Table 8 compares some related previous studies and the present study in terms of LED power, heat sink material, $T_{j,max}$ and cost. Many previous studies on LED cooling show that LED power, distances between LED chips, heat sink material, geometric parameters of the heat sink, and cooling method are effective parameters in the design of heat sinks. Copper and aluminum are the most preferred heat sink materials due to their good thermal conductivity. However, it can be said that aluminum is preferred more because it is cost effective. The maximum junction temperature of an LED is a critical parameter that defines the highest temperature the LED's semiconductor junction can reach without causing damage or negatively affecting its performance. It's essential to manage the junction temperature to ensure the LED operates within its specified limits for optimal efficiency and longevity. It is always necessary to take into account the data sheet or specifications provided by the LED manufacturer for the specific $T_{j,max}$ value of a particular LED model; because this value can vary significantly. Operating the LED within the recommended temperature range ensures reliable and efficient performance. In this study, an optimum point was selected in terms of heat sink cost and maximum led junction temperature, and an improvement was performed for the radial heat sink designed for COB LEDs.

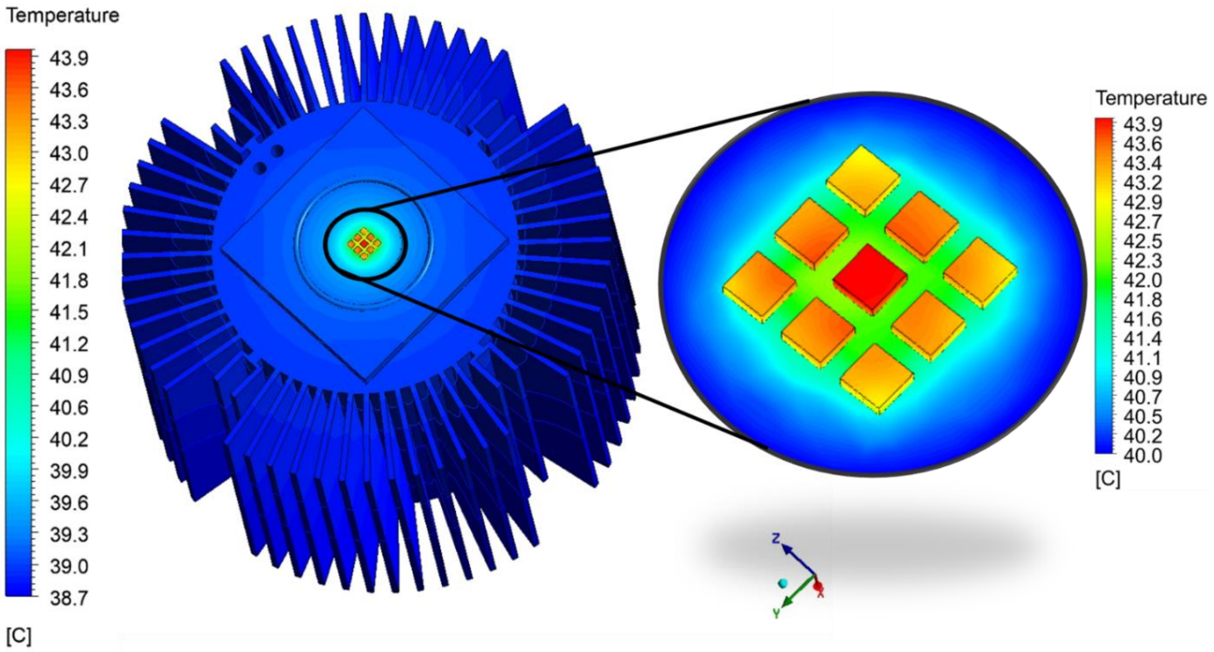

Figure 5. Validation of the optimum design.

Table 8. Comparison of the present study with some previous studies.

	LED power (W)	Heat sink material	$T_{j,max}$ (°C)	Cost ($)
Yu et al. [23]	12.37	Aluminum	64.5	N/A
Xu [6]	92	Aluminum	67.7	3.92
Wu et al. [14]	7.94	Aluminum	75.09	N/A
This study	7.94	Aluminum	43.89	0.93

4. Conclusion and Suggestions

In the present study, a Circuit on Board (COB) high power Light Emitted Diode (LED) with a radial heat sink is modeled and numerically analyzed. Besides, a multi-objective optimization for the modeled radial heat sink is introduced using the Desirability Function Approach (DFA). Maximum junction temperature ($T_{j,max}$) and radial heat sink cost (C_{hs}) are two performance parameters defined as objective functions. The goal of the multi-objective optimization procedure is to reduce both chosen performance parameters. The geometrical parameters of radial heat sink base radius (R), fin length (L), and heat sink height (H) are defined as the independent variables of both objective functions. The Response Surface Method (RSM) is employed to reduce the number of Design of Experiment (DOE) samples while still obtaining an acceptable estimation of the response values. Then, Analysis of variance (ANOVA) is used to find out how well the real and representative answer equations fit together. The minimum prediction R^2 is calculated as 0.9748%, which represents a good agreement. Finally, the optimum radial heat sink design is obtained as R=25 mm, L=15 mm, and H=55.36 mm. Besides, the response values of the optimum design are validated with a 0.25% error rate using the numerical analysis method.

In future work, a more comprehensive optimization study can be done by detailing the optimization parameters. Different optimum design proposals can be presented as a result of the analyzes to be made in different environmental conditions, such as forced air flow and natural convection.

Statement of Research and Publication Ethics

The study is complied with research and publication ethics

References

[1] M. Ha and S. Graham, “Development of a thermal resistance model for chip-on-board packaging of high power LED arrays,” *Microelectron. Reliab.*, vol. 52, no. 5, pp. 836–844, 2012.

[2] H. Yang, B. Yang, J. Li, and P. Yang, “Failure analysis and reliability reinforcement on gold wire in high-power COB-LED under current and thermal shock combined loading,” *Appl. Therm. Eng.*, vol. 150, pp. 1046–1053, 2019.

[3] C.-Y. Kang, C.-H. Lin, T. Wu, P.-T. Lee, Z. Chen, and H.-C. Kuo, “A novel liquid packaging structure of deep-ultraviolet light-emitting diodes to enhance the light-extraction efficiency,” *Crystals (Basel)*, vol. 9, no. 4, p. 203, 2019.

[4] Z. Xia, S. Liang, B. Li, F. Wang, and D. Zhang, “Influence on temperature distribution of COB deep UV LED due to different packaging density and substrate type,” *Optik (Stuttg.)*, vol. 231, no. 166392, p. 166392, 2021.

[5] G. Song, D.-H. Kim, D.-H. Song, J.-B. Sung, and S.-J. Yook, “Heat-dissipation performance of cylindrical heat sink with perforated fins,” *Int. J. Therm. Sci.*, vol. 170, no. 107132, p. 107132, 2021.

[6] Z. Xu, “Thermal performance and multi-objective optimization of thermosyphon heat sinks with rectangular radial fins for high power LED lamps cooling,” *Case Stud. Therm. Eng.*, vol. 30, no. 101778, p. 101778, 2022.

[7] M. Azarifar, C. Cengiz, and M. Arik, “Thermal and optical performance characterization of bare and phosphor converted LEDs through package level immersion cooling,” *Int. J. Heat Mass Transf.*, vol. 189, no. 122607, p. 122607, 2022.

[8] Y. Jiu, H. Fan, and W. Wang, “Investigation of a novel natural convection heat sink for LEDs based on U-shaped mini-heat pipe arrays,” *Appl. Therm. Eng.*, vol. 204, no. 118000, p. 118000, 2022.

[9] M. B. Ben Hamida, M. A. Almeshaal, K. Hajlaoui, and Y. A. Rothan, “A three-dimensional thermal management study for cooling a square Light Edding Diode,” *Case Stud. Therm. Eng.*, vol. 27, no. 101223, p. 101223, 2021.

[10] Rammohan, R. Kumar, and Chandramohan, “Experimental analysis on estimating junction temperature and service life of high power LED array,” *Microelectron. Reliab.*, vol. 120, no. 114121, p. 114121, 2021.

[11] S.-H. Moon, Y.-W. Park, and H.-M. Yang, “A single unit cooling fins aluminum flat heat pipe for 100 W socket type COB LED lamp,” *Appl. Therm. Eng.*, vol. 126, pp. 1164–1169, 2017.

[12] D. H. Shin, D. K. Sohn, and H. S. Ko, “Analysis of thermal flow around heat sink with ionic wind for high-power LED,” *Appl. Therm. Eng.*, vol. 143, pp. 376–384, 2018.

[13] B. S. Lazarov, O. Sigmund, K. E. Meyer, and J. Alexandersen, “Experimental validation of additively manufactured optimized shapes for passive cooling,” *Appl. Energy*, vol. 226, pp. 330–339, 2018.

[14] H.-H. Wu, K.-H. Lin, and S.-T. Lin, “A study on the heat dissipation of high power multi-chip COB LEDs,” *Microelectronics*, vol. 43, no. 4, pp. 280–287, 2012.

[15] W. J. Minkowycz, E. M. Sparrow, and J. Y. Murthy, Eds., *Handbook of numerical heat transfer*, 2nd ed. Nashville, TN: John Wiley & Sons, 2008.

[16] M. Sosnowski, J. Krzywanski, K. Grabowska, and R. Gnatowska, “Polyhedral meshing in numerical analysis of conjugate heat transfer,” *EPJ Web Conf.*, vol. 180, p. 02096, 2018.

[17] T. W. Simpson, A. J. Booker, D. Ghosh, A. A. Giunta, P. N. Koch, and R.-J. Yang, “Approximation methods in multidisciplinary analysis and optimization: a panel discussion,” *Struct. Multidiscipl. Optim.*, vol. 27, no. 5, 2004.

[18] O. Kalkan, A. Celen, and K. Bakirci, “Multi-objective optimization of a mini channeled cold plate for using thermal management of a Li-Ion battery,” *Energy*, vol. 251, no. 123949, p. 123949, 2022.

[19] N. R. Smalheiser, *Data literacy: How to make your experiments robust and reproducible*. San Diego, CA: Academic Press, 2017.

[20] O. Kalkan, “Multi-objective optimization of a liquid metal cooled heat sink for electronic cooling applications,” *Int. J. Therm. Sci.*, vol. 190, no. 108325, p. 108325, 2023.

[21] M. Mobin, M. Mobin, and Z. Li, “Multi-response optimisation of cavitation peening parameters for improving fatigue performance using the desirability function approach,” *Int. J. Appl. Decis. Sci.*, vol. 9, no. 2, p. 156, 2016.

[22] T. Zhang and B. Yang, “Box–cox transformation in big data,” *Technometrics*, vol. 59, no. 2, pp. 189–201, 2017.

[23] S.-H. Yu, K.-S. Lee, and S.-J. Yook, “Optimum design of a radial heat sink under natural convection,” *Int. J. Heat Mass Transf.*, vol. 54, no. 11–12, pp. 2499–2505, 2011.